Journal of Medical Imaging and Radiation Oncology

RADIOLOGY—ORIGINAL ARTICLE

Supplemental value of diffusion-weighted whole-body imaging with background body signal suppression (DWIBS) technique to whole-body magnetic resonance imaging in detection of bone metastases from thyroid cancer

Yusuke Sakurai,[1,2] Hisashi Kawai,[1] Shingo Iwano,[1] Shinji Ito,[1] Hiroshi Ogawa[3] and Shinji Naganawa[1]

[1]Department of Radiology, Nagoya University Graduate School of Medicine, Nagoya, [2]Department of Radiology, Toyohashi Municipal Hospital, Toyohashi and [3]Department of Radiology, Toyota Memorial Hospital, Toyota, Japan

Y Sakurai MD, PhD; **H Kawai** PhD; **S Iwano** PhD; **S Ito** PhD; **H Ogawa** PhD; **S Naganawa** PhD.

Correspondence
Dr Yusuke Sakurai, Department of Radiology, Nagoya University Graduate School of Medicine, 65 Tsurumai, Shouwa-ku, Nagoya 466-8550, Japan.
Email: y-sakurai@med.nagoya-u.ac.jp

Conflict of interest: None.

Submitted 28 April 2012; accepted 25 September 2012.

doi:10.1111/1754-9485.12020

Abstract

Introduction: We compared the efficacy of whole-body MRI (WBMRI) with and without diffusion-weighted whole-body imaging with background body signal suppression (DWIBS) using a 3.0-T MR scanner to [18F] fluoro-2-D-glucose positron emission tomography with CT (integrated FDG-PET/CT) for the detection of bone metastases in patients with differentiated thyroid carcinoma (DTC).

Methods: We examined 23 patients (16 women, 7 men; mean age, 56; range 17–74) with DTC who had undergone total thyroidectomy and were hospitalised to receive [I-131I] therapy. All patients underwent both WBMRI with DWIBS and whole-body FDG-PET/CT. The skeletal system was classified into 13 anatomic segments and assessed for the presence of bone metastases. Bone metastases were verified when positive findings were indicated on at least two imaging modalities: post-treated [131I] whole-body scans, WBMRI without DWIBS (T1-weighted images and short-inversion time inversion recovery images), [18F]-FDG-PET and CT.

Results: Bone metastases were confirmed in 78/290 (27%) segments in 20 (87%) of 23 patients. The sensitivities for bone metastases on a segment basis using WBMRI with DWIBS, WBMRI without DWIBS and integrated FDG-PET/CT were 64 of 78 (82%), 50 of 78 (64%) and 62 of 78 (79%), respectively; the difference between values of WBMRI with and without DWIBS was statistically significant ($P = 0.0015$). The overall accuracies of WBMRI with DWIBS, WBMRI without DWIBS and integrated FDG-PET/CT were 273 of 290 (94%), 261 of 290 (90%) and 272 of 290 (94%), respectively; the difference between values of MRI with and without DWIBS was also statistically significant ($P = 0.003$). There were only one to three false positive segments and the difference among specificities was not statistically significant in these modalities.

Conclusion: Adding DWIBS improved the sensitivity and the overall accuracy of WBMRI using 3.0-T MRI for the detection of bone metastases in patients with DTC. There was no statistically significant difference in diagnostic accuracy between MRI with DWIBS and integrated FDG-PET/CT.

Key words: [18F] fluoro-2-D-glucose positron emission tomography with computed tomography (FDG-PET/CT); bone metastasis; differentiated thyroid carcinoma; diffusion-weighted whole-body imaging with background body signal suppression (DWIBS); whole-body MRI (WBMRI).

Introduction

Differentiated thyroid carcinoma ((DTC); papillary and follicular) is characterised by good prognosis in comparison with carcinomas in other organs. The 10-year survival rate of DTC is 80% because of treatments such as total thyroidectomy and ablation of remnants with [131I] therapy.[1] However, metastases of thyroid carcinoma develop in 7–23% of patients and the overall survival rate of 10 years after a distant metastasis drops to about 40%.[1] The distant metastases occur commonly in the lungs and bone, with bone as the second most common site.[2] Patients with bone metastasis tend to do worse than those with lung metastasis.[3] Also, poor prognosis of a patient with bone metastasis is linked to the bulkiness of the lesions because the response rates of [131I] therapy decrease when the lesions are visible on radiographs.[1,4] Therefore, it is very important to detect bone metastasis in earlier stage in DTC patients.

Skeletal imaging by [18F] fluoro-2-D-glucose positron emission tomography with CT (integrated FDG-PET/CT) is useful for the detection of bone metastases from carcinomas of various organs including the thyroid gland.[5–7] Alternatively, whole-body MRI (WBMRI) has been recognised as another imaging modality for assessment of bone metastases in patients with various malignancies[8–10] and can be acquired without radiation exposure. Recently, it has been suggested that diffusion-weighted whole-body imaging with background body signal suppression (DWIBS), introduced by Takahara *et al*.,[11] can improve the detectability of bone metastasis.[5,12] Higher field strength 3.0-T MR scanners provide a higher signal-to-noise ratio (SNR) and greater spatial resolution than 1.5-T scanners.[13] Until now, many of the DWIBS techniques have used MR systems operating at 1.5 T.[5,12,14,15] At 3.0 T, not so many studies have been reported with respect to DWIBS.[16–18] No direct comparison has been made between the efficacy of WBMRI with DWIBS on 3.0-T MRI systems and that of integrated FDG-PET/CT for bone metastasis assessment of DTC patients.

The purpose of this study was to compare WBMRI with and without DWIBS using 3.0-T MRI and FDG-PET/CT in the detection of bone metastases of DTC.

Methods

Subjects

All procedures followed the clinical guidelines of Nagoya University Hospital and were approved by the Institutional Review Board. Written consent was obtained after a complete description of the study was given to all patients and their relatives. From May 2007 to December 2009, 84 patients with DTC underwent [131I] therapy at Nagoya University Hospital, 23 of whom were suspected to have bone metastasis and were selected for this study. The physicians suspected bone metastasis according to the clinical history, symptom, stage of progression, etc. All patients underwent WBMRI with DWIBS and whole-body FDG-PET/CT to detect bone metastases. Both WBMRI and whole-body FDG-PET/CT were performed prior to radioiodine therapy, and the interval between WBMRI and whole-body FDG-PET/CT was a median of 15 days (range 3–60 days). At the start of the study, 15 (65%) of the 23 patients had received previous [131I] therapy and 7 (30%) patients had undergone radiation for bone metastasis. All subjects received post-treatment [131I] whole-body scans (TxWBSs) within a median of 7 days (range 6–8 days) after treatment. Seventeen (74%) of the 23 patients had follicular carcinoma and six (26%) patients had papillary carcinomas.

Magnetic resonance imaging protocol

Magnetic resonance imaging was performed with a 3.0-T MRI scanner (MAGNETOM Trio A Tim System; Siemens AG, Erlangen, Germany) and WBMRIs were obtained with a body matrix coil and circularly polarized body array coil. Three pulse sequences were used for WBMRI. T1-weighted spin-echo sequence (relaxation/repetition time (TR)/echo time (TE), 500/11; time of acquisition, 169 s) and short-inversion time inversion recovery (STIR) turbo spin-echo sequence (TR/TE/time to inversion (TI), 6170/105/200; echo train length, 15; echo space, 6.97 ms; time of acquisition, 174 s) were acquired in the coronal plane (field of view, 500 × 500 mm; matrix, 384 × 276; slice thickness, 5 mm; slice gap, 1 mm). The overlap among each station was 70 mm. Coronal images acquired in matching positions were automatically aligned to generate a seamless whole-body image. DWIBS images were obtained in the axial plane with a spin-echo single-shot echo planar imaging with STIR incorporating the modified sensitivity encoding algorithm for parallel acquisition.[19] The parameters were as follows: TR/TE/TI, 4000/78/250; field of view, 440 × 275 mm; matrix,128 × 128; receiver bandwidth, 1502 Hz/pixel; slice thickness, 6 mm; slice gap, 6 mm; number of average, 8; time of acquisition, 46 s. Motion probing gradient pulses were applied along the superior–inferior axis with *b*-values of 800 s/mm^2. STIR was used for fat suppression. The slice-selection gradient reversal method of fat suppression was not implemented.[20] Axial whole-body MR scans were performed at seven contiguous stations with 18 interleaved 6-mm slices acquired at each station. Total acquisition time for DWIBS was about 330 s. Three-dimensional maximum intensity projection (3D-MIP) images were reconstructed from the axial DWIBS images. On all three sequences, we did not apply any respiratory compensation technique.

FDG-PET/CT examination

All FDG-PET/CT examinations were performed with a commercially available PET/CT scanner (*Biograph 16*; Siemens AG). Patients fasted for at least 6 h prior to intravenous administration of [18F]-FDG at a dose of 3.7 MBq/kg bodyweight (BW) (for BW $\leq$ 60 kg) or 4.07 MBq/kg BW (BW $>$ 60 kg), and images were obtained from the skull to the mid-thigh 50 min following FDG injection. Computed tomography was performed from the skull to mid-thigh according to a standardised protocol with the following settings: 120 kV; tube rotation time, 0.5 s per rotation; beam pitch, 20/23; section thickness, 5 mm. Patients maintained normal shallow respiration during the acquisition of CT scans and no iodinated contrast media were administered. Immediately after the unenhanced CT, PET was performed in the identical transverse field of view. The acquisition time was 1.7 min per table position. All the examinations were performed within seven to eight table positions. The resulting PET and CT scans were coregistered automatically on the workstation.

Standard of reference

The presence of bone metastases was assessed in 13 bone segments: skull, cervical, thoracic and lumbar spines, sacrum with coccyx, right and left pelvis, sternum, right and left scapulae with clavicles, right and left ribs, and upper and lower extremities.[7] At least two experienced radiologists diagnosed bone metastases using TxWBS, WBMRI (T1-weighted image and STIR image), [18F]-FDG-PET and CT. The presence of bone metastases was verified if the positive findings for bone metastases were obtained in a minimum of two imaging modalities (Fig. 1). The eight bone segments indicated a

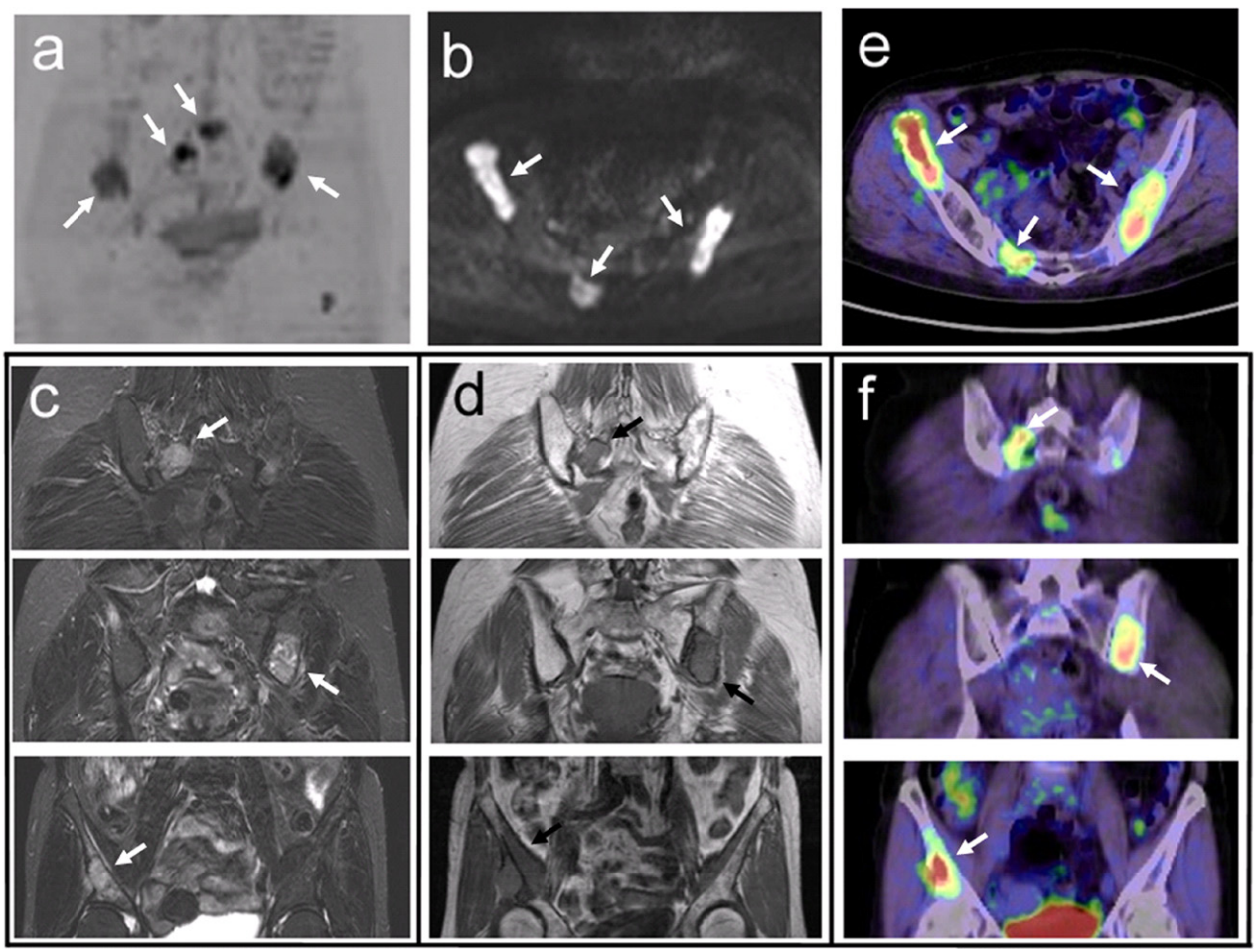

Fig. 1. A 62-year-old woman with bone metastasis of right and left pelvis, sacrum and left thigh bone. Lesions in pelvis and sacrum (arrows) are clearly demonstrated in all the following modalities: (a) diffusion-weighted whole-body imaging with background body signal suppression (DWIBS) three-dimensional maximum intensity projection images; (b) DWIBS axial image; (c) short-inversion time inversion recovery coronal images; (d) T1-weighted images; (e) [18F] fluoro-2-D-glucose positron emission tomography with CT (FDG-PET/CT) fusion axial image; and (f) FDG-PET/CT fusion coronal images.

Table 1. Distribution of metastases per bone segment

Bone segment	Number of metastases	Numbers of bone segments included
Cervical spines	5	22
Thoracic spines	10	22
Lumbar spines	7	22
Sacrum with coccyx	6	23
Right pelvis	7	22
Left pelvis	12	22
Sternum	5	22
Right scapulae with clavicles	4	23
Left scapulae with clavicles	3	23
Right ribs	7	23
Left ribs	5	22
Skull	2	21
Upper and lower extremities	5	23
Total	78	290

positive finding for metastases in only one modality and were excluded. In one patient, a metastasis was shown in the skull but was out of the scan in integrated FDG-PET/CT. Among the total of 299 bone segments examined, nine segments (3%) were excluded for these reasons.

Twenty (87%) of the 23 study patients were diagnosed with bone metastases, and 78 bone segments were confirmed to have at least one metastatic lesion according to the definitions of this study. The distribution of metastases in the examined bone segments is given in Table 1. No metastases were found in the upper and lower extremities except the thigh bone.

Image interpretation

Firstly, WBMRIs without DWIBS (T1-weighted images and STIR images) were analysed independently and separately by two radiologists with 16 and 9 years of experience, respectively. Each stack was observed initially in the coronal plane. Then, over a month later, adding DWIBS (axial plane and 3D-MIP image), WBMRIs were analysed again. The readers were blinded to the results of the other imaging technique and clinical information. Based on morphology and signal intensity, the readers were asked to assign bone segments as having metastasis or not. Each reader noted the location of the respective lesion on an analysis sheet specifically designed for this purpose. The lesions were only categorised according to the subjectively rated signal pattern, signal intensity and morphology. We did not use threshold levels for the size of lesions. On MRI, a lesion was considered to be malignant when there was a focal or a diffuse hypointense bone marrow signal compared with adjacent muscle on T1-weighted images, with a corresponding intermediate or hyperintense signal on STIR imaging, which could not be explained by a degenerative, inflammatory or traumatic cause.[21] Areas of low signal intensity on both T1-weighted and STIR sequences were interpreted as sclerosis. Furthermore, criteria for malignancy were paraosseous tumour infiltration or, for evaluation of the spine, signal changes extending into the pedicles and bulging of the anterior or posterior margin of the vertebral body. Criteria for the benign nature of a lesion were high signal intensity on T1-weighted images or a location near joint surfaces or degenerative changes of the vertebral end plates. Mild heterogeneous bone marrow changes were considered to be inhomogeneous fatty replacement of red marrow or recovering marrow. On DWI, a lesion was considered malignant when there was a focal or diffuse intermediate or high intensity without taking into account the apparent diffusion coefficients. On the other hand, a lesion was considered benign when it was located directly adjacent to degenerative changes of vertebral end plates or near joint surfaces or when it did not display high signal intensity on DWI.[12] A final consensus reading was performed between both readers if the decision was not identical.

Whole-body FDG-PET/CT fusion images were analysed in coronal, sagittal and axial planes separately and under blinded conditions by two nuclear medicine physicians with 11 and 5 years of experience, respectively. The bone segments were assigned as having metastasis or not. Here, too, the increased uptake pattern of the identified lesions was rated according to the following criteria. We used threshold levels 10 mm for the size of lesions. On PET-CT images, malignancy was defined by a focally increased FDG uptake, unless explained by other conditions, such as degenerative processes, adequate trauma or signs of infection. Using morphological information in the diagnostic CT, malignant lesions were suggested by the presence of lytic, sclerotic or mixed lytic-sclerotic intramedullary changes or bone lesions with accompany-

ing adjacent soft tissue abnormality. In the spine, lesions located at the posterior part of the body or at the pedicles were considered to be malignant, whereas lesions located at the facet joints, end plates or posterior aspect of the spinous process were considered benign.[10] No quantitative measurements were considered.

Statistical analysis

To compare the diagnostic capability on a per segment basis, McNemar's test was used to compare the sensitivity, specificity and accuracy of WBMRI with and without DWI and integrated FDG-PET/CT in overall group, prior treated ([131I] therapy and/or radiation therapy) group and non-treated group, respectively. A kappa statistic was used to determine the inter-modality agreement for the three modalities. We also compared the sensitivity of WBMRI with and without DWI and integrated FDG-PET/CT in each segment. A P value less than 0.05 was considered statistically significant for all analyses. Statistical analyses were performed using Excel 2003 (Microsoft Co., Redmond, WA, USA) with the statistical add-in software for Microsoft Excel 'Statcel' (OMS Ltd, Tokyo, Japan, 2004).

Results

Table 2 shows the distribution of metastatic deposits of all 23 patients and how three modalities performed on image interpretation.

As indicated in Table 3, in overall group, 50 (64%) of the 78 metastases were detected by WBMRI without DWIBS, and 64 (82%) of the 78 metastases were detected by WBMRI with DWIBS. The difference between these values was statistically significant ($P = 0.0015$). Sixty-two (79%) of the 78 metastases were detected by integrated FDG-PET/CT; the difference in the sensitivity between WBMRI with DWIBS and integrated FDG-PET/CT was not statistically significant ($P = 1$). The accuracy of WBMRI with DWIBS (273/290, 94%) was also higher than that of WBMRI without DWIBS (261/290, 90%); the difference between these values was statistically significant ($P = 0.003$) (Table 2). The accuracy between WBMRI with DWIBS (273/290, 94%) and integrated FDG-PET/CT (272/290, 94%) was not statistically significant.

As also shown in Table 3, there were only one to three false positive segments of the 212 bone segments that were confirmed to have no bone metastases, and the differences among specificities were not statistically significant in these modalities.

Both in non-treated group and prior treated group, the sensitivity of WBMRI without DWIBS was lower than that of WBMRI with DWIBS.

Inter-modality agreement for WBMRI with and without DWIBS (kappa = 0.83), WBMRI with DWIBS and FDG-PET/CT (kappa = 0.97) and WBMRI without DWIBS and FDG-PET/CT (kappa = 0.83) were rated substantial. WBMRI with DWIBS and FDG-PET/CT showed higher agreement than WBMRI without DWIBS.

The sensitivities of those three modalities in each segment are shown in Table 4. The difference between the sensitivities of MRI with and without DWIBS in the segment 'spines' was statistically significant (86% vs. 59%; $P = 0.04$). In the pelvis, sternum and ribs, the sensitivities of WBMRI with DWIBS were higher than those without DWIBS although significant statistical differences were not seen.

Discussion

This investigation demonstrated that WBMRI with DWIBS could be used for assessment of bone metastasis in DTC patients. The sensitivity, specificity and accuracy of WBMRI with DWIBS were equal to those of integrated FDG-PET/CT. In addition, WBMRI has several advantages over FDG-PET/CT. Firstly, WBMRI does not require any radiation exposure, whereas FDG-PET/CT generally exposes the patient to a dose of 25 mSv.[22] Secondly, WBMRI does not require fasting because the MRI scans are not affected by blood glucose. Thirdly, WBMRI does not necessitate an injection or waiting time between injection and scan. Fourthly, WBMRI seems to be more economical than FDG-PET/CT (the cost of WBMRI is only one-sixth that of FDG-PET/CT on Japanese health insurance system). Therefore, WBMRI with DWIBS might be a substitute for PET/CT to detect bone metastases of thyroid cancer.

In our study, WBMRI without DWIBS showed significantly lower sensitivity and accuracy than FDG-PET/CT. This result disagrees with past comparative studies suggesting that the efficacy of WBMRI without DWIBS for assessment of bone metastases was equal to or greater than that of FDG-PET/CT.[8–10,23] This discrepancy may be due to the localisation of bone metastasis. In our study, WBMRI without DWIBS detected significantly lower metastases in spines than WBMRI with DWIBS. In our image interpretation, the sagittal MRI images of the spine were not used and this might have resulted in the lower sensitivity of WBMRI without DWIBS. In addition, WBMRI seems to have disadvantages in detecting metastasis located in the skull and curved flat bones, especially in the thoracic cage where additional motion artefacts of respiration and pulsation impair image quality.[24,25] In our study, metastases in sternum and ribs were detected less frequently by WBMRI without DWIBS than those with DWIBS although there were not significant differences between them. These improvements might be mainly due to high contrast-to-noise ratio of lesions in DWIBS because the images of DWIBS were distorted compared with other WBMRI sequences. In addition, these might be partly due to the additional anatomical information by the different acquisition plane (DWIBS, axial; WBMRI, coronal).

Table 2. The distribution of metastatic deposits of all 23 patients and how three modalities performed on image interpretation. Each cells represent for the bone segments for each patients. Cells with 'X' mean the excluded segments. Cells with grey shadow mean the segments with bone metastases. The number '1' means true positive, '0' means false negative and the asterisk means false positive on each modalities. In the column 'modality', 'W + D' and 'W – D' mean WBMRI with and without DWIBS and 'P' means FDG-PET/CT

Bone segments	Modality	Non-treated						Prior treated																
		1	2	3	4	5	6	7	8	9	10	11	12	13	14	15	16	17	18	19	20	21	22	23
Cervical spines	W – D	0					0	0	0		0	X												
	W + D	1					0	1	1		1													
	P	0					1	0	0		1													
Thoracic spines	W – D	1	X				1		1		1		*		1	0	1			1		0	1	
	W + D	1					1		1		1		*		1	1	1			1		1	0	
	P	1					1		1		1				1	1	0			1		1	0	
Lumbar spines	W – D	1	0				1		1		1				0	1								X
	W + D	1	1				1		1		1				1	0								
	P	1	0				1		1		1				1	1								
Sacrum with coccyx	W – D	1	1				1				1	0											1	
	W + D	1	1				1				1	0											1	
	P	1	1				1				1	1											1	
Right pelvis	W – D	1					1		1	1	1				1	X				1				
	W + D	1					1		1	1	1				1					1		*		
	P	1					1		0	1	1				1					1				
Left pelvis	W – D	1	0	0			1				0	1			1	1		X		1	1		0	0
	W + D	1	1	1			1				1	1			1	1				1	1		1	1
	P	1	0	1			1				1	1			1	1				1	1		1	1
Sternum	W – D	1					0				0	1			X						0			
	W + D	1					1				1	1									0			
	P	1					1				1	1								*	0			
Right scapulae with clavicles	W – D						1				1									0	1			
	W + D						1				1									0	1			
	P						1				1									0	1			
Left scapulae with clavicles	W – D			0						1	0													
	W + D			0						1	0													
	P			0						1	0													
Right ribs	W – D	1					1				1					0				0	1	1		
	W + D	1	*				1				1					0				1	1	1		
	P	1					1				1					1				1	1	1		
Left ribs	W – D			X			1	0			1				0		0							
	W + D						1	0			1				1		1							
	P						1	1			1				1		1							
Skull	W – D										X	0						0			X			
	W + D											0						0						
	P											0						0						
Upper and lower extremities	W – D	1					1				1		1							1				
	W + D	1					1				0		1							0				
	P	1					1				0		0					*		1				

DWIBS, diffusion-weighted whole-body imaging with background body signal suppression; FDG-PET/CT, fluoro-2-D-glucose positron emission tomography with CT; WBMRI, whole-body MRI.

Table 3. Comparison of diagnostic capability of whole-body MRI (WBMRI) with and without diffusion-weighted whole-body imaging with background body signal suppression (DWIBS) and [18F] fluoro-2-D-glucose positron emission tomography with CT (FDG-PET/CT) in overall group, prior treated group and non-treated group

	WBMRI without DWIBS	WBMRI with DWIBS	FDG-PET/CT
Overall			
Sensitivity (%)	50/78 (64)†	64/78 (82)	62/78 (79)
Specificity	211/212 (100)	209/212 (99)	210/212 (99)
Accuracy	261/290 (90)†	273/290 (94)	272/290 (94)
Prior treated			
Sensitivity (%)	32/53 (60)†	41/53 (77)	41/53 (77)
Specificity	160/161 (99)	159/161 (99)	159/161 (99)
Accuracy	192/214 (90)†	200/214 (93)	200/214 (93)
Non-treated			
Sensitivity (%)	18/25 (72)	23/25 (92)	21/25 (84)
Specificity	51/51 (100)	50/51 (98)	51/51 (100)
Accuracy	69/76 (91)	73/76 (96)	72/76 (95)

†Significant difference between WBMRI without DWIBS and WBMRI with DWIBS, FDG-PEC/CT.

In the present study, the addition of whole-body DWIBS to WBMRI significantly improved sensitivity and accuracy for assessment of bone metastases. Other studies also have reported that adding DWI to WBMRI improved the detection of bone metastasis.[5,12] Wu *et al*. reported in a systematic review and meta-analysis that DWI seems to be a very sensitive but rather unspecific modality for the detection of whole-body tumour involvement because of the high heterogeneity for the specificities.[26] Therefore, DWIBS alone might not be effective to detect bone metastases. However, DWIBS shows only lesions of suspicious metastases and does not indicate any other objects including normal bones, soft tissues and organs. This means that DWIBS may be suitable to detect metastatic lesions in the whole body.[27] Therefore, additional whole-body DWIBS to WBMRI could improve sensitivity significantly.

From a technical perspective, 3.0-T MR scanners provide a higher SNR and greater spatial resolution than 1.5-T scanners.[13] Mürtz *et al*. reported that DWIBS at 3.0 T provided a better lesion-to-bone tissue contrast compared with DWIBS at 1.5 T.[16] However, this investigation also indicated that larger susceptibility-induced image distortion and signal intensity losses, stronger blurring artefacts and more pronounced motion artefacts degraded DWIBS image quality at 3.0 T. In our study, due to a high contrast-to-noise ratio, DWIBS helped detect subtle lesions and pathologic changes in normal-sized structures, and the sensitivity and accuracy of WBMRI, which provides anatomical information, were both improved by adding DWIBS.

Our study had several limitations. Firstly, the interval between WBMRI and integrated FDG-PET/CT (at most 2 months) was rather long. However, this may have little effect on the findings as DTC is a relatively slow-growing disease. Secondly, we were unable to perform a biopsy of all skeletal metastases determined by the routine examinations, so this study did not have a pathological standard of reference. However, the standard of reference we chose was the most effective method to determine lesions as we incorporated multiple imaging modalities and followed up clinically. However, we must

Table 4. Sensitivities of each segment of whole-body MRI (WBMRI) with and without diffusion-weighted whole-body imaging with background body signal suppression (DWIBS) and [18F] fluoro-2-D-glucose positron emission tomography with CT (FDG-PET/CT)

	WBMRI without DWIBS (%)	WBMRI with DWIBS (%)	FDG-PET/CT (%)
Spines	13/22 (59)†	19/22 (86)†	16/22 (73)
Sacrum with coccyx	5/6 (83)	5/6 (83)	6/6 (100)
Right and left pelvis	14/19 (74)	19/19 (100)	17/19 (89)
Sternum	2/5 (40)	4/5 (80)	4/5 (80)
Right and left scapulae with clavicles	4/7 (57)	4/7 (57)	4/7 (57)
Right and left ribs	7/12 (58)	10/12 (83)	12/12 (100)
Skull	0/2 (0)	0/2 (0)	0/2 (0)
Upper and lower extremities	5/5 (100)	3/5 (60)	3/5 (60)

†Significant difference between WBMRI without DWIBS and WBMRI with DWIBS (*P* value = 0.04).

acknowledge that our standards of reference included both WBMRI without DWIBS and integrated FDG-PET/CT, which might lead to a potential bias. Thirdly, 17 patients had already received prior [131I] therapy and/or external radiation therapy for bone metastases. This might have had a slight effect on both the images of DWIBS and FDG-PET/CT. Fourthly, we analysed the results as bone segments instead of each metastatic lesion in order to calculate specificities and accuracies. Fifthly, because the smaller lesion (less than 10 mm) was not seen in this study, it was unclear whether MRI at 3.0 T afforded better spatial resolution compared with FDG-PET/CT.

In conclusion, WBMRI with DWIBS acquired on 3.0-T MRI systems and used for bone metastasis assessment of DTC patients was found to be as sensitive and accurate as integrated FDG-PET/CT. In addition, when whole-body DWIBS was used as an adjunct for WBMRI without whole-body DWIBS, the sensitivity and accuracy of whole-body MR examination can be improved.

References

1. Schlumberger MJ. Papillary and follicular thyroid carcinoma. *N Engl J Med* 1998; **338**: 297–306.
2. Lee J, Soh EY. Differentiated thyroid carcinoma presenting with distant metastasis at initial diagnosis clinical outcomes and prognostic factors. *Ann Surg* 2010; **251**: 114–9.
3. Sampson E, Brierley JD, Le LW, Rotstein L, Tsang RW. Clinical management and outcome of papillary and follicular (differentiated) thyroid cancer presenting with distant metastasis at diagnosis. *Cancer* 2007; **110**: 1451–6.
4. Schlumberger M, Challeton C, De Vathaire F *et al*. Radioactive iodine treatment and external radiotherapy for lung and bone metastases from thyroid carcinoma. *J Nucl Med* 1996; **37**: 598–605.
5. Laurent V, Trausch G, Bruot O, Olivier P, Felblinger J, Régent D. Comparative study of two whole-body imaging techniques in the case of melanoma metastases: advantages of multi-contrast MRI examination including a diffusion-weighted sequence in comparison with PET-CT. *Eur J Radiol* 2010; **75**: 376–83.
6. Maas M, Rutten IJ, Nelemans PJ *et al*. What is the most accurate whole-body imaging modality for assessment of local and distant recurrent disease in colorectal cancer? A meta-analysis : imaging for recurrent colorectal cancer. *Eur J Nucl Med Mol Imaging* 2011; **38**: 1560–71.
7. Ito S, Kato K, Ikeda M *et al*. Comparison of 18F-FDG PET and bone scintigraphy in detection of bone metastases of thyroid cancer. *J Nucl Med* 2007; **48**: 889–95.
8. Antoch G, Vogt FM, Freudenberg LS *et al*. Whole-body dual-modality PET/CT and whole-body MRI for tumor staging in oncology. *JAMA* 2003; **290**: 3199–206.
9. Kumar J, Seith A, Kumar A *et al*. Whole-body MR imaging with the use of parallel imaging for detection of skeletal metastases in pediatric patients with small-cell neoplasms: comparison with skeletal scintigraphy and FDG PET/CT. *Pediatr Radiol* 2008; **38**: 953–62.
10. Schmidt GP, Schoenberg SO, Schmid R *et al*. Screening for bone metastases: whole-body MRI using a 32-channel system versus dual-modality PET-CT. *Eur Radiol* 2007; **17**: 939–49.
11. Takahara T, Imai Y, Yamashita T, Yasuda S, Nasu S, Van Cauteren M. Diffusion weighted whole body imaging with background body signal suppression (DWIBS): technical improvement using free breathing, STIR and high resolution 3D display. *Radiat Med* 2004; **22**: 275–82.
12. Nakanishi K, Kobayashi M, Nakaguchi K *et al*. Whole-body MRI for detecting metastatic bone tumor: diagnostic value of diffusion-weighted images. *Magn Reson Med Sci* 2007; **6**: 147–55.
13. Miao H, Fukatsu H, Ishigaki T. Prostate cancer detection with 3-T MRI: comparison of diffusion-weighted and T2-weighted imaging. *Eur J Radiol* 2007; **61**: 297–302.
14. Gutzeit A, Doert A, Froehlich JM *et al*. Comparison of diffusion-weighted whole body MRI and skeletal scintigraphy for the detection of bone metastases in patients with prostate or breast carcinoma. *Skeletal Radiol* 2010; **39**: 333–43.
15. Heusner TA, Kuemmel S, Koeninger A *et al*. Diagnostic value of diffusion-weighted magnetic resonance imaging (DWI) compared to FDG PET/CT for whole-body breast cancer staging. *Eur J Nucl Med Mol Imaging* 2010; **37**: 1077–86.
16. Mürtz P, Krautmacher C, Träber F, Gieseke J, Schild HH, Willinek WA. Diffusion-weighted whole-body MR imaging with background body signal suppression: a feasibility study at 3.0 Tesla. *Eur Radiol* 2007; **17**: 3031–7.
17. Xu X, Ma L, Zhang JS *et al*. Feasibility of whole body diffusion weighted imaging in detecting bone metastasis on 3.0T MR scanner. *Chin Med Sci J* 2008; **23**: 151–7.
18. Mürtz P, Kaschner M, Träber F *et al*. Diffusion-weighted whole-body MRI with background body signal suppression: technical improvements at 3.0 T. *J Magn Reson Imaging* 2011; **35**: 456–61.
19. Romaneehsen B, Oberholzer K, Müller LP, Kreitner KF. Rapid musculoskeletal magnetic resonance imaging using integrated parallel acquisition techniques (IPAT) – initial experiences. *Rofo* 2003; **175**: 1193–7.
20. Nagy Z, Weiskopf N. Efficient fat suppression by slice-selection gradient reversal in twice-refocused diffusion encoding. *Magn Reson Med* 2008; **60**: 1256–60.
21. Vanel D, Bittoun J, Tardivon A. MRI of bone metastases. *Eur Radiol* 1998; **8**: 1345–51.
22. Brix G, Lechel U, Glatting G *et al*. Radiation exposure of patients undergoing whole-body dual-modality

18F-FDG PET/CT examinations. *J Nucl Med* 2005; **46**: 608–13.
23. Yi CA, Shin KM, Lee KS *et al*. Non-small cell lung cancer staging: efficacy comparison of integrated PET/CT versus 3.0-T whole-body MR imaging. *Radiology* 2008; **248**: 632–42.
24. Daldrup-Link HE, Franzius C, Link TM *et al*. Whole-body MR imaging for detection of bone metastases in children and young adults: comparison with skeletal scintigraphy and FDG PET. *AJR Am J Roentgenol* 2001; **177**: 229–36.
25. Walker R, Kessar P, Blanchard R *et al*. Turbo STIR magnetic resonance imaging as a whole-body screening tool for metastases in patients with breast carcinoma: preliminary clinical experience. *J Magn Reson Imaging* 2000; **11**: 343–50.
26. Wu LM, Gu HY, Zheng J *et al*. Diagnostic value of whole-body magnetic resonance imaging for bone metastases: a systematic review and meta-analysis. *J Magn Reson Imaging* 2011; **34**: 128–35.
27. Kwee TC, Takahara T, Ochiai R, Nievelstein RA, Luijten PR. Diffusion-weighted whole-body imaging with background body signal suppression (DWIBS): features and potential applications in oncology. *Eur Radiol* 2008; **18**: 1937–52.